# First-principles calculations of the effect of pressure on the iron-based superconductor LaFeAsO

Hiroki Nakamura* and Masahiko Machida†
*CCSE, Japan Atomic Energy Agency, 6-9-3 Higashi-Ueno, Taito, Tokyo 110-0015, Japan;*
*JST, Transformative Research-Project on Iron Pnictides (TRIP), Chiyoda, Tokyo 102-0075, Japan;*
*and CREST–JST, 4-1-8 Honcho, Kawaguchi, Saitama 332-0012, Japan*
(Received 2 August 2009; published 7 October 2009)

We perform first-principles calculations for an iron-based superconductor LaFeAsO in order to study its pressure effects. As the pressure increases, we find a change from monotonic to nonmonotonic shrinking manner in lattice constants and related crystalline parameters at 20 GPa and a structural transition from the orthorhombic to the tetragonal crystal with a disappearance of the antiferromagnetically ordered moment at 24 GPa in an excellent agreement with an experimental observation. Moreover, the calculations reveal that the structural transition is almost the phase transition of the second order. We further explore a very high-pressure range and find that the contraction of the distance between As and Fe plane stops above 100 GPa although the *c*-axis lattice constant continues to shrink.

DOI: 10.1103/PhysRevB.80.165111 PACS number(s): 74.62.Fj, 71.15.Mb, 74.25.Jb, 74.70.−b

Since the discovery of the iron-based superconductor $LaFeAsO_{1-x}F_x$ whose critical temperature is 26 K,[1] a tremendous number of studies have been made on the research of its superconducting mechanism and properties. So far, the highest critical temperature has exceeded 50 K,[2] and several authors have therefore proposed unconventional mechanisms.

The crystal structures of discovered iron-based superconductors are now mainly classified into four types by their structural differences of nonsuperconducting blocking layers, i.e., LnFeAsO(1111), $AFe_2As_2$(122),[3] LiFeAs(111),[4] and $\alpha$-FeSe(11).[5] In addition to these four types, a new one whose blocking layer structure is a perovskite type has been very recently reported.[6,7] These rich varieties may promise further advancement toward higher $T_c$ and more useful superconductors.

A similarity among these compounds is Fe *Pn* (*Pn*=As, P, or Se) layer structure, which is a stage exhibiting high-$T_c$ superconductivity. The element, As, P, or Se lies on the top of the pyramid distant by $h_{As}$ from the center of the square lattice formed by four Fe atoms. The material properties including the superconductivity are known to be very sensitively dependent on the distance $h_{As}$. Several authors actually have argued that the magnetic moment and the density of states (DOS) around the Fermi surface drastically change by a tiny shift of $h_{As}$.[8–10] In this paper, we study pressure effects of a parent compound LaFeAsO and reconfirm the sensitivity through the observed pressure effects.

In order to obtain high-$T_c$ superconductivity, most of these parent compounds require carrier doping via chemical substitution such as $LaFeAsO_{1-x}F_x$ or deficiency introduction such as $PrFeAsO_{1-x}$. This is very similar to cuprate high-$T_c$ superconductors. On the other hand, there are different ways unlike cuprates in iron-based superconductors. One way is the direct doping on Fe-As layer, as seen in $FeSe_{1-x}$ and $LaFe_{1-x}Co_xAsO$, and another way is the direct pressure application on the parent compounds. Especially, the latter is very convenient for first-principles calculations because one can systematically examine the changes in the electronic structure without changing supercells depending on the doping ratio. Thus, we study the pressure effects on a parent compound LaFeAsO by using the same unit cell and clarify how the system responds to the pressure variation.

LaFeAsO does not show the superconducting transition under ambient pressure while its critical temperature reaches 20 K around 12 GPa.[11] This pressure-induced superconductivity is also observed in the case of $CaFe_2As_2$,[12] $SrFe_2As_2$ ($T_c \sim 30$ K around 4 GPa),[13,14] $EuFe_2As_2$ ($T_c=30$ K around 3 GPa),[15,16] and $BaFe_2As_2$ ($T_c=29$ K around 4 GPa).[14] On the other hand, in optimally doped materials exhibiting superconductivity at ambient pressure, the pressure changes their critical transition temperatures. $LaFeAsO_xF_{1-x}$ exhibits the critical temperature enhancement from 26 to 43 K up to 5 GPa,[17] while $T_c$ of $SmFeAsO_xF_{1-x}$ decreases monotonically with increasing the pressure.[18,19] $T_c$ of FeSe also increases up to around 30 K.[20,21] According to these findings, we expect a ground-state phase diagram like Fig. 1(a). In this paper, we focus on a nondoped material and fully study the transition from the magnetically ordered phase by first-principles calculations.

There have been several theoretical works on the pressure

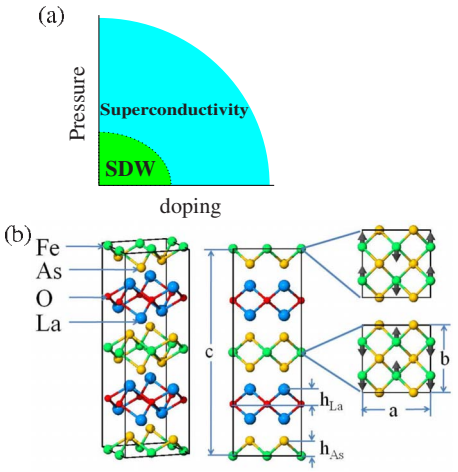


FIG. 1. (Color online) (a) A schematic ground-state phase diagram of typical iron-based superconductors. (b) The crystal structure of LaFeAsO. The bold arrows show the direction of the magnetic moment of iron atoms.

 

TABLE I. Lattice constants and other parameters at zero pressure. The errors from experimental data are shown in the parentheses. The experimental data are taken from Ref. 24.

| | $a$ (Å) | $b$ (Å) | $c$ (Å) | $h_{\mathrm{As}}$ (Å) | $h_{\mathrm{La}}$ (Å) |
|---|---|---|---|---|---|
| Experiment | 5.7096 | 5.6818 | 17.4524 | 1.3080 | 1.2444 |
| Magnetic | 5.7579 | 5.6912 | 17.4292 | 1.2744 | 1.2403 |
| | (0.85%) | (0.17%) | (−0.13%) | (−2.59%) | (−0.33%) |
| NonMagnetic | 5.6878 | 5.6878 | 17.2308 | 1.1903 | 1.2498 |

effects in iron-based superconductors. Among them, we particularly mention two previous first-principles studies.[22,23] Our results are consistent with the previous works while more precise and wide investigations are done in our calculations. For instance, we adopt 1 GPa pressure step around the transition point and explore a much wider pressure range up to 200 GPa.

The crystal structure of LaFeAsO examined in this paper is displayed in Fig. 1(b). At the room temperature, this compound is paramagnetic under a tetragonal crystal structure. As the temperature decreases, a transition into the orthorhombic crystal structure occurs and the stripe-type magnetic order successively develops. Then, the crystal structure belongs to the space group *Ibam* as seen in Fig. 1(b). Table I shows a comparison of the unit lengths along the principal axes and other parameters among an experiment[24] and two types of calculations at the ambient pressure. The difference between the two types of calculations (called magnetic and nonmagnetic) is whether one takes into account the spin degree of freedom or not. The lattice constants, $a$, $b$, and $c$ under the magnetically ordered structure are in agreement with the experimental data within 1% error. On the other hand, if one does the nonmagnetic calculation, then the stable structure is automatically the tetragonal one and $c$ becomes worse than that of the magnetic calculation as shown in Table I. As for $h_{\mathrm{As}}$, the magnetic calculation shows a better agreement with the experimental data than the nonmagnetic case. However, the error of $h_{\mathrm{As}}$ is relatively larger ($\sim$−2.59%) than errors of other parameters as seen in Table I. It is noted that even if the structure becomes tetragonal by doping or raising the temperature, the observed $h_{\mathrm{As}}$ is almost unchangeable, i.e., $h_{\mathrm{As}} \sim 1.3$ Å. This unexpected error may be an origin of various disagreements with the experiments.

The calculation package employed throughout this paper is VASP,[25] which uses projector-augmented wave method[26] and generalized gradient approximation exchange-correlation energy.[27] $K$ points are taken as $8\times8\times8$ and the electronic self-consistent loop is repeated until the energy difference between loops becomes less than $10^{-6}$ eV. The crystal structure is stabilized until the atomic forces are reduced to less than 0.01 eV/Å. We obtain the pressure value directly from the calculated stress tensor in contrast to the previous works.[22,23]

The magnetic calculation well reproduces the observed structure except for $h_{\mathrm{As}}$, whereas it has been well known that the antiferromagnetically ordered moment per an iron atom shows a large deviation from the experimental results. The calculated moment is $\sim 2.0\mu_{\mathrm{B}}$ while the experimental one is $\sim 0.3\mu_{\mathrm{B}}$.[24,28,29] Several explanations on this discrepancy have been suggested. For instance, one of the suggestions is that spin fluctuations around a quantum critical point can make the observed moment smaller. However, this inconsistency with the density-functional theory (DFT) is much beyond our theoretical expectation. Another suggestion is that polarization effects of As are underestimated.[10,30] This may be related with a wrong agreement of $h_{\mathrm{As}}$. On the other hand, Mazin *et al.*,[31] proposed that the first-principles calculation is valid while antiferromagnetic domain fluctuations effectively suppress the static moment. In fact, high-frequency optical phonons excited inside Fe-As layers are well reproducible under the moment $2.0\mu_{\mathrm{B}}$.[32] Moreover, the observed spin dynamical structure factor in neutron experiments shows a strong magnetic excitation peak around 10 meV and relatively broad weights over a wide range frequency above 10 meV.[33] This means that static experiments such as Mössbauer effects cannot directly measure the large iron magnetic moment. If this scenario is correct, then DFT estimates the value of the iron moment integrated over the frequency range correctly, i.e., DFT reasonably predicts a larger moment than the observed one as the static moment. Thus, we believe that our results are qualitatively correct, and therefore, the first-principles calculation on the pressure effects is worth studying. Of course, DFT cannot explain why the dynamical spin structure factor has finite weights over such a wide range of frequency. In this paper, we avoid further discussion on the moment value and perform the standard DFT calculation. Thus, our main goal is not a perfect quantitative agreement but a qualitative understanding of pressure-induced phenomena.

Now, let us show calculation results of the pressure effects. The first focus is how the crystal structures change as a function of the pressure. Figure 2 shows lattice constants and other parameters related to the crystal structure vs the external hydrostatic pressure in which nonmagnetic calculation results are also plotted for comparison. Since the tetragonal symmetry is always stable in the nonmagnetic calculation, the pressure effects are monotonic in all the pressure range. Concentrating on the lattice structural parameters in the magnetic calculation, we notice that clear irregularities emerge at 24 GPa,[34] above which all the magnetic calculation results completely coincide with the nonmagnetic ones. Thus, the structural phase transition from orthorhombic to tetragonal is clearly found to occur at 24 GPa. In addition, the magnetic calculations reveal that the lattice constants and the related ones change from monotonic behaviors to nonmonotonic rapid ones at 20 GPa. In particular, a drastic decreasing slope change in $h_{\mathrm{As}}$ at 20 GPa, which is an almost kink like, brings about a rapid change in the electronic structure as shown

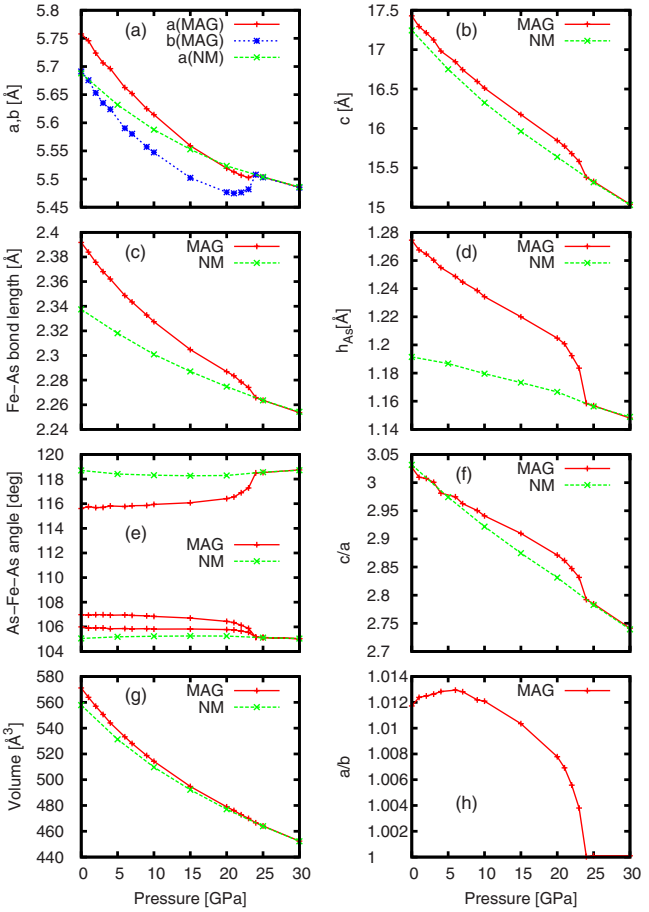


FIG. 2. (Color online) Pressure dependence of (a) lattice constants $a$ and $b$, (b) $c$, (c) Fe-As bond length, (d) $h_{As}$, (e) As-Fe-As angles, (f) ratio of lattice constants, $c$ and $a$, (g) volume of unit cell, and (h) ratio of $a$ and $b$. MAG corresponds to results obtained by the magnetic calculation and NM to nonmagnetic calculation.

below [see also Figs. 3(a), 3(b), and 4]. In other words, the rapid change is a precursor of the phase transition at 24 GPa. Generally, we expect a sudden jump, i.e., the first-order transition for structural phase transition but the present one is not the case. This is confirmed by the pressure dependences of the volume [Fig. 2(g)] and the energy [Fig. 3(c)].

Let us turn back to the results below 20 GPa. Contrary to those above 20 GPa, the lattice constants $a$, $b$, $c$, $h_{As}$, and Fe-As bond length decrease monotonically with increasing the pressure up to 20 GPa. The three As-Fe-As angles are almost constant below 20 GPa. These results mean that this material simply shrinks up to 20 GPa. On the other hand, we notice that the shrink ratio along $c$ axis is larger than that of $a$ axis. This tendency is easily found by $c/a$ ratio as function of the pressure shown in Fig. 2(f). This is quite consistent with the experimental results.[13] Furthermore, we find around 6 GPa that $a/b$ reaches the maximum as shown in Fig. 2(h). This indicates that the crystal structure is the farthest from the tetragonal structure at 6 GPa. With increasing the pressure from the ambient one, once the crystal structure anisotropy increases, it becomes the maximum around 6 GPa, and changes into the decreasing behavior toward the transition to the tetragonal one.

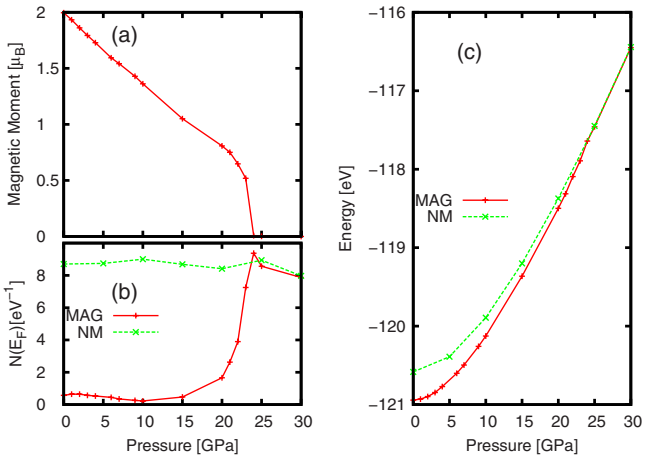


FIG. 3. (Color online) (a) Magnetic moment of an iron atom and (b) density of states at the Fermi energy as a function of pressure. (c) The ground-state energy as a function of pressure.

Now, let us concentrate on the structural phase transition at 24 GPa again. The volume of the unit cell looks smooth at this critical pressure in spite of the nonmonotonic change in each lattice constant from 20 to 24 GPa. This is because the rapid expansion of $b$ just cancels out the shrinkage of $c$. This clearly indicates that the in-plane structural variation is tightly connected with that of the out of plane. In Fig. 3(a), the magnetic moment of an iron atom decreases as the pressure increases, and vanishes at the same pressure as the orthorhombic-to-tetragonal transition (24 GPa). The moment disappearance at 24 GPa shows a very good quantitative agreement with an observation data of Mössbauer effect.[35] As mentioned above, one may presume that our results are quantitatively wrong due to the overestimated magnetic moments at ambient pressure. Nevertheless, it is not surprising that the result shows a good agreement with the observed data. Under such a high pressure, almost all the phonons are harden, i.e., high-energy structural fluctuations are suppressed, and then the dynamically fluctuating spin coupled with the structural fluctuation is pushed into a lower-frequency range. This indicates that the DFT static calcula-

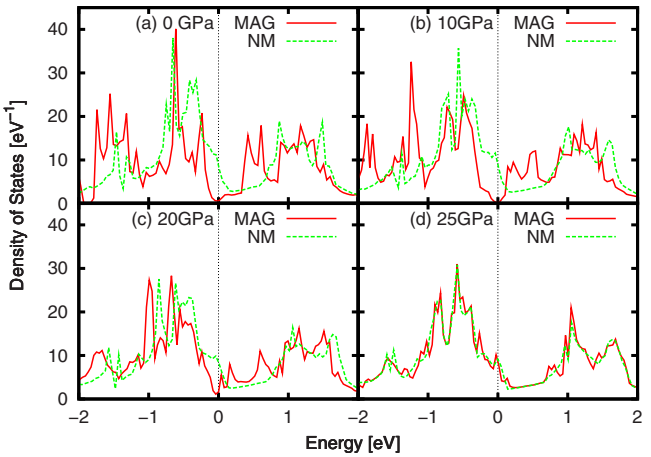


FIG. 4. (Color online) Density of states at various pressures. The Fermi energy is set to zero.

tion result approaches closer to the experimental value under high-pressure application. As shown in Fig. 3(b) the DOS rapidly increases above 20 GPa and shows a peak slightly below the transition. The reason why DOS rapidly develops is that the Fermi surface turns into that of the nonmagnetic case without a pseudogap such as DOS suppression. This behavior can be also reproducible by adjusting the moment value.[36] Figure 3(c) is the ground-state energy vs the pressure. Below 24 GPa, the ground-state energy of the magnetic calculation is always lower than that of the nonmagnetic one. At 24 GPa, their energy values cross in a continuous manner and the ground state is replaced by the nonmagnetic one with the tetragonal phase above 24 GPa. From these energy and volume [Fig. 2(g)] variations, it is found that the transition is the second order. This result implies that fluctuations associated with the transition are rather enhanced in the pressure-induced case.

Figure 4 shows DOS at various pressure values around 20 GPa. In a relatively low-pressure range, (a) 0 and (b) 10 GPa, where the Fe moment is still large, there exists a pseudogap such as DOS suppression at the Fermi energy.[37] The gap width correlates with the moment value. As the pressure increases, the pseudogap shrinks and finally disappears just at 24 GPa, where the magnetic moment vanishes and the magnetic DOS almost coincides that of the nonmagnetic one as seen in (d). This pressure-induced pseudogap closing is in a qualitative agreement with the pressure dependence of the resistivity.[13]

The final is pressure effects under considerably high pressure. The motivation comes from an expectation that a new phase might emerge under such an unexplored pressure range. We increase the pressure up to 200 GPa. The results, i.e., the lattice constants $a$ and $c$ vs the pressure are shown in Fig. 5(a). We find that both constants monotonously shrink with increasing the pressure. On the other hand, $h_{\mathrm{As}}$ above 100 GPa shrinks no longer while the crystal components irrelevant to $h_{\mathrm{As}}$ continues to contract. This result indicates highly asymmetry potential curve for $h_{\mathrm{As}}$. Thus, we find no significant change in the electronic structure from 24 to 200 GPa. In addition, as for angles of As-Fe-As [Fig. 5(c)] we do not also observe any drastic changes.

In summary, we evaluated pressure dependences of various properties of iron-based superconductor LaFeAsO by DFT calculations. We found that as the pressure increases above 20 GPa the magnetic moment immediately decreases with associated nonmonotonic structural variations and vanishes at 24 GPa being consistent with the experiment. Furthermore, we explored a very high-pressure range up to 200 GPa and found that $h_{\mathrm{As}}$ shrinks no longer above 100 GPa in contrast to the unceasing volume contraction.

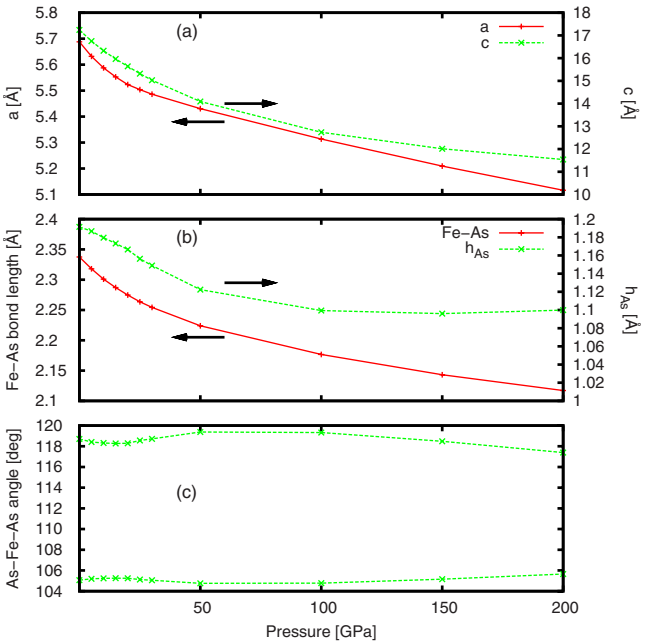


FIG. 5. (Color online) (a) Lattice constants, (b) Fe-As bond length and $h_{\mathrm{As}}$, and (c) As-Fe-As angles as a function of higher pressure.

The authors wish to thank H. Takahashi, T. Kawakami, and H. Okada for providing their recent experimental results and K. Terakura and N. Hamada for illuminating discussion in first-principles calculations. The authors also thank S. Shamoto, A.Q.R. Baron, T. Fukuda, J. Mizuki, T. Tohyama, T. Morinari, N. Hayashi, Y. Nagai, M. Okumura, and N. Nakai for valuable discussion. The work was partially supported by Grant-in-Aid for Scientific Research on Priority Area "Physics of new quantum phases in superclean materials" (Grant No. 20029019) from the Ministry of Education, Culture, Sports, Science and Technology of Japan.

*nakamura.hiroki@jaea.go.jp
†machida.masahiko@jaea.go.jp

[1] Y. Kamihara, T. Watanabe, M. Hirano, and H. Hosono, J. Am. Chem. Soc. **130**, 3296 (2008).
[2] C. Wang, L. Li, S. Chi, Z. Zhu, Z. Ren, Y. Li, Y. Wang, X. Lin, Y. Luo, S. Jiang, X. Xu, G. Cao, and Z. Xu, EPL **83**, 67006 (2008).
[3] M. Rotter, M. Tegel, and D. Johrendt, Phys. Rev. Lett. **101**, 107006 (2008); K. Sasmal, B. Lv, B. Lorenz, A. M. Guloy, F. Chen, Y.-Y. Xue, and C. W. Chu, *ibid.* **101**, 107007 (2008).
[4] J. H. Tapp, Z. Tang, B. Lv, K. Sasmal, B. Lorenz, P. C. W. Chu, and A. M. Guloy, Phys. Rev. B **78**, 060505(R) (2008).
[5] F.-C. Hsu, J.-Y. Luo, K.-W. Yeh, T.-K. Chen, T.-W. Huang, P. M. Wu, Y.-C. Lee, Y.-L. Huang, Y.-Y. Chu, D.-C. Yan, and M.-K. Wu, Proc. Natl. Acad. Sci. U.S.A. **105**, 14262 (2008).
[6] H. Ogino, Y. Matsumura, Y. Katsura, K. Ushiyama, S. Horii, K. Kishio, and J. Shimoyama, Supercond. Sci. Technol. **22**, 075008 (2009).
[7] X. Zhu, F. Han, G. Mu, P. Cheng, B. Shen, B. Zeng, and H.-H. Wen, Phys. Rev. B **79**, 220512(R) (2009).
[8] I. I. Mazin, M. D. Johannes, L. Boeri, K. Koepernik, and D. J. Singh, Phys. Rev. B **78**, 085104 (2008).

[9] F. Yndurain and J. M. Soler, Phys. Rev. B **79**, 134506 (2009).
[10] K. Kuroki, H. Usui, S. Onari, R. Arita, and H. Aoki, Phys. Rev. B **79**, 224511 (2009).
[11] H. Okada, K. Igawa, H. Takahashi, Y. Kamihara, M. Hirano, H. Hosono, K. Matsubayashi, and Y. Uwatoko, J. Phys. Soc. Jpn. **77**, 113712 (2008).
[12] M. S. Torikachvili, S. L. Bud'ko, N. Ni, and P. C. Canfield, Phys. Rev. Lett. **101**, 057006 (2008).
[13] H. Takahashi, H. Okada, K. Igawa, K. Arii, Y. Kamihara, S. Matsuishi, M. Hirano, H. Hosono, K. Matsubayashi, and Y. Uwatoko, J. Phys. Soc. Jpn. **77**, Suppl. C, 78 (2008).
[14] P. L. Alireza, Y. T. C. Ko, J. Gillett, C. M. Petrone, J. M. Cole, G. G. Lonzarich, and S. E. Sebastian, J. Phys.: Condens. Matter **21**, 012208 (2009).
[15] C. F. Miclea, M. Nicklas, H. S. Jeevan, D. Kasinathan, Z. Hossain, H. Rosner, P. Gegenwart, C. Geibel, and F. Steglich, Phys. Rev. B **79**, 212509 (2009).
[16] T. Terashima, M. Kimata, H. Satsukawa, A. Harada, K. Hazama, S. Uji, H. S. Suzuki, T. Matsumoto, and K. Murata, J. Phys. Soc. Jpn. **78**, 083701 (2009).
[17] H. Takahashi, K. Igawa, K. Arii, Y. Kamihara, M. Hirano, and H. Hosono, Nature (London) **453**, 376 (2008).
[18] B. Lorenz, K. Sasmal, R. P. Chaudhury, X. H. Chen, R. H. Liu, T. Wu, and C. W. Chu, Phys. Rev. B **78**, 012505 (2008).
[19] Y. Takabayashi, M. T. McDonald, D. Papanikolaou, S. Margadonna, G. Wu, R. H. Liu, X. H. Chen, and K. Prassides, J. Am. Chem. Soc. **130**, 9242 (2008).
[20] Y. Mizuguchi, F. Tomioka, S. Tsuda, T. Yamaguchi, and Y. Takano, Appl. Phys. Lett. **93**, 152505 (2008).
[21] S. Margadonna, Y. Takabayashi, Y. Ohishi, Y. Mizuguchi, Y. Takano, T. Kagayama, T. Nakagawa, M. Takata, and K. Prassides, Phys. Rev. B **80**, 064506 (2009).
[22] S. Lebegue, Z. P. Yin, and W. E. Pickett, New J. Phys. **11**, 025004 (2009).
[23] Y. Yang and X. Hu, arXiv:0903.5113 (unpublished).
[24] C. de la Cruz, Q. Huang, J. W. Lynn, W. Jiying Li, I. I. Ratcliff, J. L. Zarestky, H. A. Mook, G. F. Chen, J. L. Luo, N. L. Wang, and P. Dai, Nature (London) **453**, 899 (2008).
[25] G. Kresse and J. Hafner, Phys. Rev. B **47**, 558 (1993); G. Kresse and J. Furthmüller, Comput. Mater. Sci. **6**, 15 (1996); Phys. Rev. B **54**, 11169 (1996).
[26] P. E. Blöchl, Phys. Rev. B **50**, 17953 (1994); G. Kresse and D. Joubert, *ibid.* **59**, 1758 (1999).
[27] J. P. Perdew, K. Burke, and M. Ernzerhof, Phys. Rev. Lett. **77**, 3865 (1996).
[28] S. Kitao, Y. Kobayashi, S. Higashitaniguchi, M. Saito, Y. Kamihara, M. Hirano, T. Mitsui, H. Hosono, and M. Seto, J. Phys. Soc. Jpn. **77**, 103706 (2008).
[29] H.-H. Klauss, H. Luetkens, R. Klingeler, C. Hess, F. J. Litterst, M. Kraken, M. M. Korshunov, I. Eremin, S.-L. Drechsler, R. Khasanov, A. Amato, J. Hamann-Borrero, N. Leps, A. Kondrat, G. Behr, J. Werner, and B. Buchner, Phys. Rev. Lett. **101**, 077005 (2008).
[30] G. A. Sawatzky, I. S. Elfimov, J. van den Brink, and J. Zaanen, EPL **86**, 17006 (2009).
[31] I. I. Mazin and M. D. Johannes, Nat. Phys. **5**, 141 (2009).
[32] T. Fukuda *et al.* (unpublished).
[33] M. Ishikado, R. Kajimoto, S. Shamoto, M. Arai, A. Iyo, K. Miyazawa, P. M. Shirage, H. Kito, H. Eisaki, S. W. Kim, H. Hosono, T. Guidi, R. Bewley, and S. M. Bennington, J. Phys. Soc. Jpn. **78**, 043705 (2009).
[34] The predicted transition pressure in Ref. 23 is 29 GPa. This difference is caused by the accuracy. Their pressure bin can be estimated as 5–6 GPa from their volume bin $0.02V/V_0$, while ours is 1 GPa. Their result is consistent with ours within the margin of error.
[35] T. Kawakami, T. Kamatani, H. Okada, H. Takahashi, S. Nasu, Y. Kamihara, M. Hirano, and H. Hosono (private communication).
[36] H. Nakamura, N. Hayashi, N. Nakai, and M. Machida, J. Phys. Soc. Jpn. **77**, Suppl. C, 153 (2008).
[37] See, e.g., S. Ishibashi, K. Terakura, and H. Hosono, J. Phys. Soc. Jpn. **77**, 053709 (2008).